



Influence of snow surface processes on soil moisture dynamics and streamflow generation in alpine catchments

Nander Wever^{1,2}, Francesco Comola¹, Mathias Bavay², and Michael Lehning^{2,1}

¹ École Polytechnique Fédérale de Lausanne (EPFL), School of Architecture, Civil and Environmental Engineering, Lausanne, Switzerland.

² WSL Institute for Snow and Avalanche Research SLF, Davos, Switzerland.

Correspondence to: Nander Wever (wever@slf.ch)

Abstract. The assessment of flood risks in alpine, snow covered catchments requires an understanding of the linkage between the snow cover, soil and discharge in the stream network. Here, we apply the comprehensive, distributed model Alpine3D to investigate the role of soil moisture in the predisposition of a catchment to high flows from rainfall and snow melt for the Dischma catchment in East Switzerland. The recently updated soil module of the physics based, multi-layer snow cover model SNOWPACK, which solves the surface energy and mass balance in Alpine3D, is verified against soil moisture measurements at seven sites and various depths inside and in close proximity of the Dischma catchment. Measurements and simulations in such terrain are difficult and consequently, soil moisture was simulated with varying degrees of success. Differences between simulated and measured soil moisture mainly arises from an overestimation of soil freezing and an absence of a ground water description in the model. Both were found to have an influence in the soil moisture measurements. Streamflow simulations performed with a spatially-explicit hydrological model using a travel time distribution approach coupled to Alpine3D provided a closer agreement with observed streamflow at the outlet of the Dischma catchment when including 30 cm of soil layers. Performance decreased when including 2 cm or 60 cm of soil layers. This demonstrates that the role of soil moisture is important to take into account when understanding the relationship between both snowpack runoff and rainfall and catchment discharge in high alpine terrain. Runoff coefficients (i.e., ratio of rainfall over discharge) based on measurements for high rainfall and snowmelt events were found to be dependent on the simulated initial soil moisture state at the onset of an event, further illustrating the important role of soil moisture for the hydrological processes in the catchment. The runoff coefficients using simulated discharge were found to reproduce this dependency and this shows that the Alpine3D model framework can be successfully applied to assess the predisposition of the catchment to flood risks from both snowmelt and rainfall events.

1 Introduction

Alpine catchments are sensitive to flooding events (*Frei et al.*, 2000), with positive contributing factors being, for example, the topography, high rainfall rates and shallow soil depths (*Weingartner et al.*, 2003). The presence of a snow cover, acting as a water storage over winter, may dampen flood risks during some parts of the year (*Weingartner et al.*, 2003), but also provides an important contribution to catchment scale runoff via meltwater in spring. Correct estimations of snow cover and snowmelt distributions are therefore essential for accurate streamflow simulations (*Maurer and Lettenmaier*, 2003; *Berg and Mulroy*,



2006; Seyfried *et al.*, 2009; Koster *et al.*, 2010). Additionally, rain-on-snow events may significantly increase the liquid water outflow from the snowpack (Mazurkiewicz *et al.*, 2008; Wever *et al.*, 2014a; Würzer *et al.*, 2016) and many flooding events have been caused by such events (Marks *et al.*, 2001; Rössler *et al.*, 2014).

However, accurate simulations of liquid water draining from the snowpack due to snowmelt or rainfall (henceforth termed snowpack runoff) are not sufficient to understand catchment runoff. The degree of saturation of the soil was found to determine the eventual effect of snowpack runoff on streamflow (McNamara *et al.*, 2005; Seyfried *et al.*, 2009; Bales *et al.*, 2011). This effect is not limited to snowpack runoff, but is also found for rainfall (Bales *et al.*, 2011; Penna *et al.*, 2011). During the winter months, the snow cover basically decouples the soil from the atmosphere and the upper boundary for the soil is determined by the state of the snow cover on top (McNamara *et al.*, 2005; Kumar *et al.*, 2013). Often, the hydrological processes are strongly reduced during winter time, such as groundwater flow and streamflow, until the spring snowmelt provides liquid water again to the hydrological system. A model system to assess the hydrological response of a catchment is therefore required to simulate both the soil and the snowpack accurately.

To assess this coupling between snowmelt, soil moisture and streamflow, the use of physics based models of snow surface process descriptions in hydrological models seems attractive as they should not require calibration for the specific application. For example, Rigon *et al.* (2006) show that the physics based hydrological model GEOtop, which includes a relatively simple physics based snow scheme, is able to provide accurate streamflow simulations for small catchments, where a snow cover is present for extended periods during the winter season. Kumar *et al.* (2013) also found that using a physics based model approach for snow related processes in the PIHM model achieved a slightly better performance for streamflow simulations than a temperature index approach. The results in their study suggest that this improvement is linked to the spatial variability of snow distribution and snowmelt, which provides a strong control on other components of the hydrological cycle, like soil moisture or streamflow. In Warscher *et al.* (2013), a similar comparison was made by comparing a temperature-index approach with an energy balance approach to determine snowmelt in the physics based hydrological model WaSiM-ETH. Their results show that the energy balance approach provides improvements particularly at the small spatial scales typical of high alpine headwater catchments. However, the improvements rapidly decrease with increasing scale. It has been argued that simple temperature index based snowmelt models may perform well after careful calibration (Kumar *et al.*, 2013; Comola *et al.*, 2015a) and those models are still commonly used in operational flood forecasting. Nevertheless, physics based snow models may be considered more reliable when extrapolating to other conditions such as for climate change scenarios (e.g., Bavay *et al.* (2013)) or to catchment where limited calibration data is available.

The fully-distributed Alpine3D model is typically applied for detailed studies of small scale surface processes in alpine catchments where snow plays an important role (Lehning *et al.*, 2006; Mott *et al.*, 2008; Groot Zwaaftink *et al.*, 2013). In this study, the recent addition to the SNOWPACK model of a solver for Richards Equation for soil (see Wever *et al.* (2014a, 2015)) is verified against soil moisture measurements in the vicinity of Davos, Switzerland. The SNOWPACK model additionally provides a physics based description of soil-snow-vegetation processes in the Alpine3D model framework (Gouttevin *et al.*, 2015). Here, the capabilities of Alpine3D to capture the soil moisture state and its influence on streamflow generation in the catchment is assessed.



2 Study Area and Data

2.1 Study Area

The Davos area is located in the Canton Graubünden in east Switzerland. The studied area is defined as an area of $21.5 \times 21.5 \text{ km}^2$ and stretches over an elevation range from about 1250 m above sea level (a.s.l.) to 3218 m a.s.l. Some small glaciers exist in the highest parts, covering about 0.86 km^2 (Zappa *et al.*, 2003). The Dischma catchment is an unregulated catchment in the Davos area and has been subject to previous studies concerning streamflow from the Dischma river (e.g., Zappa *et al.* (2003); Lehning *et al.* (2006); Bavay *et al.* (2009); Schaepli *et al.* (2014); Comola *et al.* (2015b)). The measurement site Weissfluhjoch (WFJ), which is focussed on snow-related measurements, is located in close proximity of the area, as well as several permanent meteorological stations. Figure 1 shows the studied area, including the measurement stations and the gauging station for streamflow measurements of the Dischmabach in the Dischma catchment. Streamflow data has been provided by the Swiss Federal Office for the Environment (FOEN). Simulations presented in this study consist of three winter seasons, from October 1, 2010 to September 30, 2013.

Snowfall plays an important role in the Davos area. Table 1 shows the precipitation sums for two heated rain gauges at two elevations in the region. About 40% to 80% of all precipitation falls as snow at the lower and upper parts of the Dischma catchment, respectively (Zappa *et al.*, 2003). The winter months are dominated by snowfall at all elevations in the area. In the meteorological summer months (June–August), about 25% of the precipitation amounts still consist of snowfall at 2536 m a.s.l. At the lower rain gauge, almost all precipitation falls as rain in the meteorological summer months. There exists a strong elevation gradient in precipitation: at 2536 m a.s.l., precipitation amounts are about 1.9 times higher than at 1590 m a.s.l. This elevation gradient may, however, overestimate the true areal-mean gradient because the upper site may be limited representative for the Dischma catchment (Wirz *et al.*, 2011; Grünewald and Lehning, 2015). Furthermore, the area exhibits a climatological northwest - southeast gradient in precipitation (not shown).

Figures 2a and 2b show the daily temperature and precipitation amounts separated in snowfall and rainfall, for both locations with a heated rain gauge. The yearly cycle in temperature has a similar amplitude at both elevations. Maximum daily temperatures occasionally surpassed 20°C at 1590 m a.s.l. and 15°C at 2536 m a.s.l. The minimum daily temperatures reached -20°C and -25°C , respectively. Note that those low temperatures were reached after significant snowfall in the months before. Therefore, the isolating snow cover is expected to have prevented an impact of these cold days on soil freezing.

An important event in the meteorological forcing can be found in winter season 2011–2012, which was dominated by large snowfalls in December, January and February. Maximum measured snow height was higher than in the other simulated years. Cold temperatures in those months were followed by a relatively warm spring season, resulting in relatively high snowmelt rates. Also the spring of snow season 2010–2011 was relatively warm, compared to the spring of 2012–2013. None of the summer periods were outspokenly dry or wet, and precipitation occurred homogeneously distributed over time, with the exception of the dry November 2011, in which no precipitation occurred. Finally, total precipitation at WFJ in summer 2011 was similar to summer 2012, whereas the summer 2013 was rather dry in Davos.



2.2 Data

Several measurement sites are located or were temporarily installed in the vicinity of Davos. Their locations are shown in Figure 1. The sensitivity of Alpine3D simulations to input data coverage as well as specific interpolation and modelling choices is discussed in detail in *Schlögl et al. (2016)*. Here we operate with a standard set-up as described below and distinguish between the 5 types of meteorological stations (see Table 2):

(i) IMIS stations: those stations are permanently installed operational meteorological stations in the Swiss Alps, especially focussed on usage for avalanche warning (*Lehning et al., 1999*). The stations measure at 7.5 m above the ground and are designed for long-term operational use. For this purpose, they receive regular maintenance and quality control. One exception is SLF2 in Davos-Dorf, which is used as a test station for new sensors or hardware. During the winter season 2011 and for a large part of winter season 2012, the relative humidity sensor was providing erroneous data due to a faulty test sensor.

(ii) IRKIS stations: these stations were temporarily set up for this study. They are based on the IMIS design, although they are smaller than IMIS stations with a height of 4.5 m. The IRKIS stations were additionally equipped with soil moisture sensors at 10, 30, 50, 80 and 120 cm depth. At each depth, two sensors were installed at approximately 50 cm distance. The IRKIS station SLF2 was using the IMIS station SLF2, but soil moisture sensors were installed in close vicinity. IRKIS stations report weather and soil moisture conditions at a time resolution of 10 minutes.

(iii) SensorScope stations: to improve the data quantity and the area covered by measurements, SensorScope stations (*Ingelrest et al., 2010*) were installed in less accessible terrain for a period of approximately 2-3 years. Operation of these type of stations in the harsh winter conditions appeared to be more difficult than expected and the sometimes hazardous locations of the measurement sites was hindering maintenance during the winter season. Due to several outages of the stations and broken sensors, the meteorological measurement series contain many gaps and are not used as input in this study. The SensorScope stations were also equipped with soil moisture sensors at 10, 30 and 50 cm depth. At the Golf Course station, sensors were additionally installed at 80 and 120 cm depth. Also here, two sensors were installed at each depth. In this study, we consider the soil moisture data to be useful for validation. SensorScope stations measure at a time resolution of 1 minute, sending their data using GPRS cell phone networks.

(iv) SwissMetNet stations: the Swiss Federal Office of Meteorology and Climatology (MeteoSwiss) operates meteorological stations in the SwissMetNet network. In the vicinity of Davos, two SwissMetNet stations are present: at the WFJ (2536 m a.s.l.) and in Davos-Dorf (1590 m a.s.l.). They are equipped with a heated rain gauge, providing relatively accurate measurements of solid precipitation in winter, and incoming shortwave and longwave radiation sensors. At WFJ, shortwave and longwave radiation sensors located at a mountain peak of 2691 m a.s.l. were used in this study. These sensors experience almost no shadowing from surrounding mountain peaks, compared to the ones at the WFJ measurement site (see below) and could be considered more representative for the Davos area.

(v) WFJ: this measurement site serves as the main research site for the WSL Institute for Snow and Avalanche Research SLF and is focussed on snow related processes (*Marty and Meister, 2012; WSL Institute for Snow and Avalanche Research SLF, 2015-09-29*). The site is equipped with an IMIS type station, as well as a heated rain gauge that is part of the SwissMetNet



network. Furthermore, ventilated temperature and relative humidity sensors are present as well as incoming and reflected shortwave and incoming and outgoing longwave radiation sensors. Several backup sensors are present, allowing for filling data gaps.

At the soil moisture measurement sites, Decagon 10HS soil moisture sensors were installed (*Decagon Devices*, 2014).
5 *Mittelbach et al.* (2012) present an in-depth comparison with other types of soil moisture sensors. A few important issues related to the Decagon 10HS sensors that are relevant for this study were reported. In their study, the liquid water content values from the sensors exhibited a soil temperature dependency. The sensors were also found to hardly register values above $0.40 \text{ m}^3 \text{ m}^{-3}$ and it was concluded that the 10HS is showing a decreased sensitivity with increasing liquid water content. Consequently, the sensors are unable to follow fluctuations in wet soil conditions. For some of the sites and depths where we
10 installed these type of sensors, the measured LWC is around or above $0.40 \text{ m}^3 \text{ m}^{-3}$. We therefore expect a strongly reduced dynamic response in these locations. However, many of the installed sensors were recording values well below $0.40 \text{ m}^3 \text{ m}^{-3}$ and provide useful measurements. The dielectric constant of ice is much lower than for water, making the sensors mostly sensible to the liquid water content part only.

3 Methods

15 3.1 Simulation Setup

SNOWPACK is a one-dimensional physics based multi-layer snow cover model (*Lehning et al.*, 2002a, b). Richards equation (*Richards*, 1931) is used to describe soil moisture dynamics and numerically solved using finite differences scheme over the model layers (elements). Water flow in snow is solved by the bucket scheme, which provides accurate snowpack runoff estimations on daily and seasonal time scales (*Wever et al.*, 2014b), and has noticeable lower computational costs for distributed
20 simulations. The liquid water outflow from the snowpack is prescribed as the upper boundary condition for the Richards equation for the soil, which is solved in SNOWPACK as described in (*Wever et al.*, 2014b). In snow-free conditions, the upper boundary condition is defined by rainfall, evaporation and deposition resulting from the latent heat flux. Phase changes in soil are calculated following *Wever et al.* (2015). Water retention curves in the SNOWPACK model are based on the van Genuchten model (*van Genuchten*, 1980) via predefined soil types as in the ROSETTA class average parameters (*Schaap et al.*, 2001).

25 To run simulations for the Dischma catchment, the Alpine3D model system is used, which describes surface processes in complex terrain by performing distributed SNOWPACK simulations (*Lehning et al.*, 2006). For describing the high spatial variability in incoming and outgoing long and shortwave radiation, including shadowing effects and the surface reflections of shortwave radiation, a detailed energy balance module is available (*Michlmayr et al.*, 2008). An additional module considers drifting snow (*Lehning et al.*, 2008; *Mott et al.*, 2010), including sublimation processes (*Groot Zwaafstink et al.*, 2013). These
30 drifting snow modules are not used in this study, as the location of the measurement sites are not prone to significant drifting snow effects, except for the Grossalp station. Moreover, the calculation of the wind fields and snow drift is posing a high computational demand compared to the other modules. The different modules and the coupling strategy is described in *Lehning et al.* (2006).



The Alpine3D simulations were run for a domain of 21.5 km×21.5 km with a grid cell size of 100 m×100 m, giving a total size of 215 × 215 grid cells. The model was run in hourly time steps, providing meteorological forcing data per time step for each pixel by interpolating from the meteorological stations in and just outside the Davos area using the MeteIO library (Bavay and Egger, 2014). Per hourly time step, 4 SNOWPACK time steps are executed at 15 min. resolution.

5 The precipitation measurements from the heated rain gauges in Davos and WFJ were interpolated over the grid by using the elevation gradient from the measurements. The commonly used temperature threshold in the SNOWPACK model of 1.2 °C was used to separate precipitation into rain and snowfall. Air temperature, relative humidity and wind speed were also interpolated over the grid, using the station data as indicated in Table 2 and applying IDW with lapse rates calculated from the available data. Only IMIS stations were used for spatial interpolations, except for the radiation components. Incoming longwave radiation was
10 interpolated using a lapse rate between both SwissMetNet stations providing radiation. Shortwave radiation is provided by the radiation module, using the measurements from WFJ. The radiation balance is closed by the SNOWPACK simulations at each grid points, when SNOWPACK calculates the surface temperature and surface albedo.

Two important components to initialise Alpine3D simulations are the digital elevation model (DEM) for the Davos area, provided by the Swiss Federal Office of Topography (swisstopo). Also the soil has to be initialised for each pixel, although
15 limited information is available. We based soil properties on the land use classification, as provided by swisstopo (Zappa *et al.*, 2003). Table 4 lists the land use classes, the percentage of areal coverage in the simulated area and the soil initializations. Pixels that were defined as glacier, ice, firn, road, settlements, rivers and lakes (6%) were initialised in a state that represents the land use class. Other vegetation free areas are classified as rocky surface. This class is assigned to 29% of the pixels and consist for a large part of ground moraine and scree slopes, whereas solid rock and rock walls are sparse in the Davos area. The rocky surface
20 pixels were initialised uniformly with loamy sand. This is based on observations when installing soil temperature sensors at the WFJ, which is located in the rock class and for which plausible simulations were obtained using this soil class (Wever *et al.*, 2015). All other pixels (65%), including forests, meadows, pasture, bare soil, and occasional pixels that are defined as agricultural use were initialised using an upper layer of 60 cm consisting of silt loam and a lower layer of 240 cm consisting of sandy loam. This choice is based on observations when installing the soil moisture sensors at the IRKIS and SensorScope
25 stations. The soil permeability classification provided by the Swiss Federal Office for Agriculture (FOAG) shows generally high permeability in the area surrounding Davos, which confirms the choice for soil types with no clay content. To determine thermal properties of the soil, literature values were taken (Table 3). For thermal conductivity, a wide range of values is reported and a strong dependence with water content is present. We used values corresponding to typical soil saturation values, based on work by Ochsner *et al.* (2001) and Bachmann *et al.* (2001).

30 A soil depth of 3 m was simulated, subdivided into 23 layers. The layer spacing was 2 cm near the surface, increasing to 40 cm at 3 m depth. The densely spaced surface layers are necessary to describe the large gradients of temperature and moisture occurring in this region. The lower boundary condition at 3 m depth was set as a water table condition for the liquid water flow and as a constant upward geothermal heat flux of 0.06 W m⁻² for the heat equation.

For the simulations, atmospheric stability was taking into account when calculating the turbulent heat fluxes, using the
35 modified Stearns correction (Schlögl *et al.*, in review). The roughness length during the presence of a snow cover was defined



to be 0.015 m below 1900 m a.s.l. and 0.002 m otherwise. This division is based on the generally rougher terrain below 1900 m, due to the presence of trees or large bushes, whereas above 1900 m, mainly meadows and scree fields are present. When pixels are snow free, they were assigned a roughness length of 0.02 m.

Alpine3D has recently been extended with MPI support, allowing for the parallelisation of the distributed SNOWPACK and energy balance simulations. Using 36 CPU cores, the computation took on average 14 hours for a single year, mainly depending on snow height in the winter season, on a computer cluster from 2008.

3.2 Analysis

The soil moisture measurements series were first cleaned from erroneous data, like negative values, or data from broken sensors after visual inspection of the time series. Then, data was aggregated to hourly and daily time scales by calculating average soil moisture contents over the respective time spans. From the simulations, the modelled soil moisture values were extracted for each depth at which also measurements were taken. The output resolution was 1 hour and also here, daily values were calculated by averaging the hourly values.

As the area of Davos is dominated by snowfall in winter, a separation is made for yearly, summer and winter periods. The summer months are defined as the period from June through October. At the elevation of the soil moisture stations, snowfall episodes are almost absent in these months and the winter snow cover has melted completely by the beginning of June. The winter months are defined as the period from November through May, when a snow cover is present. Note that typically, the snow cover melts away in April or May at the stations and in those months, the soil moisture is expected to be strongly influenced by the snowmelt from the snowpack.

The streamflow from the Dischmabach is calculated using a streamflow model that uses a travel time distribution approach, as outlined in *Comola et al.* (2015b) and described in detail in *Gallice et al.* (2016). In this study, three inputs for the streamflow model are defined by soil water fluxes in 55 sub-catchments, taking the flux in 2, 30 or 60 cm depth, respectively. The 2 cm flux represents a case where almost all water input into the soil from both snow melt as well as rainfall is directly routed using the streamflow model, while at the same time ensuring that evaporation is taken into account. The simulations using the flux at 30 or 60 cm depth are performed to verify the sensitivity of the streamflow model to the thickness of the soil layers used in Alpine3D.

The travel time distribution approach separates the soil in an upper and lower compartment, where the upper one represents the fast response and the lower one the slow response. The method has three parameters that require calibration: the average travel time of the upper and lower soil compartment (day) and the maximum recharge rate of the lower compartment from the upper compartment (mm day^{-1}). Here, all three approaches which define the input for the streamflow model are independently calibrated with measured discharge from October 2004 to September 2009, using Monte-Carlo simulations with 5000 repetitions. The best combination of coefficients was determined based on the highest Nash-Sutcliffe Model Efficiency (NSE) coefficient (*Nash and Sutcliffe*, 1970). The period from October 2009 - September 2014 was used for validation.

To analyse the effect of soil moisture on streamflow generation, we calculated the average soil saturation in the top 40 cm of all pixels inside the Dischma catchment. Furthermore, we defined rainfall events as events for which the 12 hour sum exceeds



10 mm. The time series for the event was determined by taking the average value of both heated rain gauges. The start of the event is defined as the first time step for which precipitation is present, and the end was determined when the cumulative 12 hour sum fell below 3 mm, after first reaching 10 mm. A similar approach was done for snowpack runoff from the model, where snowpack runoff is considered analogue to rainfall.

5 4 Results and Discussion

4.1 Snow Height

Figure 3 shows measured and simulated snow depth by Alpine3D for stations SLF2, Uf den Chaiserren and Grossalp. In snow season 2011 and 2013, the snow height in the Alpine3D simulations is satisfyingly reproduced at both SLF2 and Uf den Chaiserren. The snow height at Grossalp is overestimated in all snow seasons. This is explained by the fact that this particular site is relatively sensitive to wind eroding snow from the surface. The snow depth in snow season 2012 is overestimated at all stations, which is related to unusual meteorological circumstances of large snowfalls accompanied by strong winds, which lead to an overestimation of precipitation as measured by the heated rain gauge (also discussed in *Wever et al. (2015)*). Nevertheless, the snow cover development at those three sites is overall satisfactorily simulated in Alpine3D for providing an upper boundary for the soil.

15 4.2 Soil Moisture Measurements and Simulations

Figures 4 and 5 show measured and simulated soil moisture time series at all depths for 2 of the 7 stations in the area of Davos. Similar figures for the other 5 stations can be found in the Online Supplement. Temporal variations in soil moisture in the area of Davos are clearly dominated by winter periods, in which the presence of a snow cover reduces or inhibits water influx at the top of the soil for several months. This phase is followed by the snowmelt phase in spring, when liquid water draining from the snowpack is providing liquid water again to the soil. The summer months are snow-free, and soil moisture measurements show fluctuations on short time scales of a few days, related to rainfall and evaporation.

At several stations, soil freezing is indicated by the soil moisture sensors. Significant soil freezing was occurring in snow season 2011, as clearly indicated at SLF2 (Figure 4) and Uf den Chaiserren (Figure 5), as well as Stillberg (see Figure S2 in the Online Supplement). The soil freezing was promoted by a long period with no snow or only a shallow snow cover, allowing the soil to cool. For the stations SLF2 and Uf den Chaiserren, the onset of the freezing is rather well predicted in the Alpine3D simulations. At most stations, the soil freezing front does not seem to reach the sensor at 30 cm depth. Only at Uf den Chaiserren and Stillberg, the minimum soil moisture at this depth in this particular snow season is slightly lower than in the other snow seasons, which may be indicative of slight soil freezing here.

The simulations show soil freezing at 10 cm depth in all snow seasons at most stations, for at least a short period of time, which is more soil freezing than captured in the soil moisture measurements. The overestimation of soil freezing in the simulations may be partly related to neglecting the presence of vegetation at the measurement sites. All sites are covered by



grass, or rough pasture and bushes. To account for the insulating effects of the canopy, some soil freezing schemes consider the presence of a canopy when calculating soil phase changes (e.g., *Giard and Bazile (2000)*). Due to the lack of possible validation data, we did not implement this. Furthermore, the amount of soil freezing is also dependent on the amount of liquid water available. At stations Grossalp and Golf Course, the soil is wetter than simulated, which would require a higher heat flow out of the soil before freezing may start. Finally, uncertainties in soil thermal properties may play a role.

The relatively dry summer of 2013, most pronounced at low elevations as indicated by the difference in summer precipitation from both heated rain gauges (Table 1), is clearly visible in the simulations by a drop in soil moisture at all depths, reaching the lowest values of the entire measurement period. Unfortunately, soil moisture sensors had stopped working at many stations by this time, but at the site SLF2 and Stillberg, a good correspondence is found in the 10 cm measured and simulated soil moisture series. At the Uf den Chaiserren site, the recession curve in this summer is particularly present at the sensors at 50 and 80 cm depth, and absent in the highest sensor.

Some features are found that likely relate to hydrological processes that are not simulated in the Alpine3D model. For example, at the Uf den Chaiserren site, the soil moisture at 80 and 120 cm is clearly influenced by a rising water table in the late snowmelt season. This is indicated by the sudden rise to high values of saturation, remaining constant afterwards (Figure 5). The soil at the Golf Course station appeared to be close to saturation for extended periods of time (see Figure S5 in the Online Supplement), which is congruent with observations when installing the sensors. The location of these two stations close to the Dischmabach (Uf den Chaiserren) and Landwasser river (Golf Course), which are partly fed by meltwater from the glacierised area, supports this interpretation. The apparent interaction with ground water levels at these stations is not considered in the simulations, as the ground water table is fixed at the lower boundary of the soil column in the model domain. Similarly, the measurements at 10 and 30 cm depth at the Grossalp station (see Figure S3 in the Online Supplement) also indicate high saturation of the soil, for which no source of water could be found. Due to the insensitivity of the soil moisture sensors in wet soil conditions, discrepancies between simulations and measurements as found at the sites Grossalp and Golf Course can only be assessed qualitatively and provide insights on the limitations of the measurements and simulations. In contrast with the other measurement sites, the soil moisture sensors at the Pischa station show a very dynamic response (see Figure S3 in the Online Supplement). We cannot exclude that during the installation of the sensors, the soil was disturbed in such a way that afterwards, efficient preferential flow paths occurred along the boundaries of the displaced soil layers.

Figure 6 shows the r^2 values between measured and simulated soil moisture for the various depths for the full period and for the summer months only. Here, soil moisture was taken as the sum of ice and water to compensate for the overestimation of soil freezing. Only the values for the sensor with the highest r^2 value of the two sensors per depth are shown. Generally, the highest r^2 is achieved for 30 cm and 50 cm depth. Closer to the surface, the overestimation in soil freezing, as well as the generally large gradients in soil moisture reduces the agreement. For deeper layers, ground water dynamics as discussed above, which is not considered by the model, could be identified as contributing to lower model agreement. Results for the summer months show higher r^2 values for the 10 cm and 30 cm soil moisture sensors. These layers are particularly influenced by rainfall in these months, for which timing is more accurate in the model than the onset of snowpack runoff which determines soil moisture



fluctuations in large periods of the year. For deeper layers, the model performance is comparable to the performance for the full year.

4.3 Streamflow

Figure 7 shows the measured and simulated streamflow at the outlet of the Dischmabach in the Dischma catchment. The winter periods are clearly identifiable by the hydrograph falling back to baseflow. Furthermore, high discharge is particularly found in spring, during the snowmelt season which typically lasts from April to June in the Dischma catchment (*Griessinger et al.*, 2016). During the summer period, streamflow slowly decreases, interrupted regularly with peaks in streamflow due to rainfall. These general discharge patterns are well captured in the simulations, regardless of the depth below the surface where the liquid water flux is routed to the runoff model. However, the fast dynamics on daily time scales in the Dischmabach streamflow is underestimated in the simulations, particularly when using the flux at 60 cm depth. Improvements in reproducing the dynamic response on short time scales in the simulations could probably be obtained by including lateral water transport in Alpine3D, which would allow us to account for the fast surface runoff, which for example takes place over highly saturated or impervious soils.

The three simulations of streamflow differ in the water input used for the travel time distribution approach. Figure 8 displays the NSE coefficients per year as well as the average for the three virtual lysimeters defined in the model. For the full validation period, the NSE coefficient for either the 2 cm, 30 cm or 60 cm flux provide very similar scores of around 0.8. When the calculation of NSE coefficients is limited to the snow melt season (April-June) or the summer season (June-October) only, differences become more pronounced. Highest NSE coefficient is achieved with the flux at 30 cm depth. The results suggests that the updated soil module of SNOWPACK is contributing to a better prediction of streamflow in the summer months.

We hypothesize that in the Dischma catchment, the snow melt season is providing large water fluxes from the snow to the soil, compared to the soil water dynamics, making it the dominant factor in predicting stream flow. In the summer months, however, the predisposition of the soil is also an important factor, thus neglecting the soil layers almost completely, by routing the 2 cm flux to the runoff model, is reducing the model efficiency.

4.4 Predisposition from Soil Moisture

The soil moisture state of the Dischma catchment is summarized as the basin wide average saturation in the upper 40 cm of the soil at the onset of a rainfall or snowpack runoff event. The water flux at this depth provided the highest skill in reproducing observed discharge after applying the streamflow model. Figure 9a shows the runoff coefficient (i.e., the ratio of rainfall to discharge) for the cumulative rainfall and measured discharge from the Dischma catchment as a function of catchment average soil saturation. The figure illustrates that the reduced storage capacity in wetter soils leads indeed to more of the precipitation water being routed to discharge and vice versa. In Figure 9b, it is illustrated that similar behaviour is also captured in the simulated discharge. For the Dischma catchment, we found that not only the total event runoff coefficient is determined by the soil moisture state, but also the peak runoff coefficient, defined as the ratio of the maximum peak in precipitation over the maximum, not necessarily simultaneous, discharge peak (see Fig. 9c). This relationship is again also found for the simulated



discharge (Fig. 9d). Although the initial soil moisture is impacting the runoff coefficient for both the cumulative amounts as well as the peak values, the time lag between a peak in rainfall and measured discharge is not dependent on the soil moisture conditions (Fig. 9e). Also this result is reproduced by the simulated discharge (see Fig. 9f). All r^2 values reported in Fig. 9 test significant at the 95 % confidence level.

5 When the catchment is snow-covered, the melt water outflow from the snowpack can be considered analogous to rainfall in summer. A similar analysis as presented in Fig. 9 is performed using snowpack runoff (see Fig. 10). Also here we find that the soil moisture state at the onset of snowpack runoff events influences the streamflow discharge. Similar to rainfall events, the soil moisture state influences the ratio of the cumulative measured event discharge over cumulative snowpack runoff (Fig. 10a) as well as the peak ratio (Fig. 10c). The correlation coefficients are higher for the snowpack runoff events than for the
10 rainfall events. This higher correlation coefficient for snowpack runoff than rainfall is also found for the runoff coefficients using simulated discharge (Fig. 10b and d). Similar to rainfall events, the time delay between peaks in snowpack runoff and discharge is independent of the initial soil moisture state.

The results show that the simulations of the soil moisture state contribute to the understanding of how rainfall and snowpack runoff input in the hydrological system is influencing discharge from the catchment. Based on measurement, this relationship
15 was found for alpine catchments for summer rainfall (*Penna et al.*, 2011). However, we show that this effect is reproduced in both measured runoff coefficients as well as simulated ones and also exists for snowpack runoff. The relationship between the initial soil moisture state and runoff coefficients is similar for observed and simulated discharge as well as for rainfall or snowpack runoff events. These results suggest that simulations of soil moisture in snow dominated catchments are able to provide understanding of the discharge behaviour from the catchment and is a crucial factor in assessing flood risks.

20 5 Conclusions

Simulations with the spatially explicit Alpine3D model were performed for the area of Davos. The recent update of the soil module of SNOWPACK, which is used in the Alpine3D model, shows satisfactory results for simulating soil moisture at 7
stations with soil moisture measurements in the area around Davos. The comparison included measurements at 10, 30 and 50 cm depths, and at 4 stations also at 80 and 120 cm depths. Correlation coefficients show that generally, the temporal
25 variability is adequately captured. However, often a bias between simulated and measured soil moisture was found.

In winter, the amount of soil freezing was higher in the Alpine3D simulations than indicated by the measurements. The soil moisture measurements also provide some clear indications of fluctuations in ground water level above 120 cm depth. Ground water dynamics is not taken into account in the model, as the water table was fixed to the lower boundary of the soil column in the model domain. Also uncertainties in soil properties and measurements likely play an important role in discrepancies
30 between simulations and measurements.

Relating the water flux at 30 cm depth in the soil to streamflow in the Dischma catchment using a travel time distribution approach provided a higher agreement with observed streamflow than directly using the water flux at the top of the soil or at 60 cm depth. Event and peak runoff coefficients using measured discharge were found to correlate with the simulated soil



moisture state at the onset of rainfall or snowpack runoff events. Runoff coefficients for both the event as well as the peak were higher when the soil saturation was higher and vice versa. For snowpack runoff, this effect was found to be stronger. Also runoff coefficients using simulated discharge exhibited a stronger relationship with initial soil saturation. The fact that a simulated soil moisture state could be related to the effect on measured streamflow, indicates that soil module of the SNOWPACK model in the Alpine3D model framework can successfully assess the predisposition of the catchment for flood risk assessments.

Acknowledgements

This research has been conducted in the framework of the IRKIS project supported by the Office for Forests and Natural Hazards of the Swiss Canton of Grisons (Dr. Chr. Wilhelm), the region of South Tyrol (Italy) and the community of Davos. We also thank Tobias Jonas for installing and maintaining the soil moisture measurements for stations Uf den Chaiserren, Grossalp and SLF2, and S. Valär for kindly allowing the installation of soil moisture sensors and weather stations on his property. The Alpine3D and SNOWPACK models and MeteoIO are available under a LGPLv3 license at <http://models.slf.ch>.



References

- Bachmann, J., R. Horton, T. Ren, and R. R. van der Ploeg (2001), Comparison of the thermal properties of four wettable and four water-repellent soils, *Soil Sci. Soc. Am. J.*, 65(6), 1675–1679, doi:10.2136/sssaj2001.1675.
- Bales, R. C., J. W. Hopmans, A. T. O’Geen, M. Meadows, P. C. Hartsough, P. Kirchner, C. T. Hunsaker, and D. Beaudette (2011), Soil moisture response to snowmelt and rainfall in a Sierra Nevada mixed-conifer forest, *Vadose Zone J.*, 10(3), 786–799, doi:10.2136/vzj2011.0001.
- 5 Bavay, M., and T. Egger (2014), MeteoIO 2.4.2: a preprocessing library for meteorological data, *Geosci. Model Dev.*, 7(6), 3135–3151, doi:10.5194/gmd-7-3135-2014.
- Bavay, M., M. Lehning, T. Jonas, and H. Löwe (2009), Simulations of future snow cover and discharge in Alpine headwater catchments, *Hydrol. Proc.*, 23(1), 95–108, doi:10.1002/hyp.7195.
- 10 Bavay, M., T. Grünewald, and M. Lehning (2013), Response of snow cover and runoff to climate change in high Alpine catchments of Eastern Switzerland, *Adv. Water Resour.*, 55, 4–16, doi:10.1016/j.advwatres.2012.12.009.
- Berg, A. A., and K. A. Mulroy (2006), Streamflow predictability in the Saskatchewan/Nelson River basin given macroscale estimates of the initial soil moisture status, *Hydrolog. Sci. J.*, 51(4), 642–654, doi:10.1623/hysj.51.4.642.
- Comola, F., B. Schaeffli, P. D. Ronco, G. Botter, M. Bavay, A. Rinaldo, and M. Lehning (2015a), Scale-dependent effects of solar radiation patterns on the snow-dominated hydrologic response, *Geophys. Res. Lett.*, 42(10), 3895–3902, doi:10.1002/2015GL064075, 2015GL064075.
- 15 Comola, F., B. Schaeffli, A. Rinaldo, and M. Lehning (2015b), Thermodynamics in the hydrologic response: Travel time formulation and application to Alpine catchments, *Water Resour. Res.*, 51(3), 1671–1687, doi:10.1002/2014WR016228.
- Decagon Devices (2014), 10HS soil moisture sensor, *Tech. rep.*
- Frei, C., H. Davies, J. Gurtz, and C. Schär (2000), Climate dynamics and extreme precipitation and flood events in Central Europe, *Integr. Assess.*, 1(4), 1389–5176, doi:10.1023/A:1018983226334.
- 20 Gallice, A., M. Bavay, T. Brauchli, F. Comola, M. Lehning, and H. Huwald (2016), StreamFlow 1.0: An extension to the spatially distributed snow model Alpine3D for hydrological modeling and deterministic stream temperature prediction, *Geosci. Model Dev. Discuss.*, 2016, 1–51, doi:10.5194/gmd-2016-167.
- Giard, D., and E. Bazile (2000), Implementation of a new assimilation scheme for soil and surface variables in a global NWP model, *Mon. Wea. Rev.*, 128(4), 997–1015, doi:10.1175/1520-0493(2000)128<0997:IOANAS>2.0.CO;2.
- 25 Gouttevin, I., M. Lehning, T. Jonas, D. Gustafsson, and M. Mölder (2015), A two-layer canopy model with thermal inertia for an improved snowpack energy balance below needleleaf forest (model SNOWPACK, version 3.2.1, revision 741), *Geosci. Model Dev.*, 8(8), 2379–2398, doi:10.5194/gmd-8-2379-2015.
- Griessinger, N., J. Seibert, J. Magnusson, and T. Jonas (2016), Assessing the benefit of snow data assimilation for runoff modeling in alpine catchments, *Hydrol. Earth Syst. Sci.*, 20(9), 3895–3905, doi:10.5194/hess-20-3895-2016.
- 30 Groot Zwaaftink, C. D., A. Cagnati, A. Crepez, C. Fierz, G. Macelloni, M. Valt, and M. Lehning (2013), Event-driven deposition of snow on the Antarctic Plateau: analyzing field measurements with SNOWPACK, *Cryosphere*, 7(1), 333–347, doi:10.5194/tc-7-333-2013.
- Grünewald, T., and M. Lehning (2015), Are flat-field snow depth measurements representative? a comparison of selected index sites with areal snow depth measurements at the small catchment scale, *Hydrol. Proc.*, 29(7), 1717–1728, doi:10.1002/hyp.10295.
- 35 Ingelrest, F., G. Barrenetxea, G. Schaefer, M. Vetterli, O. Couach, and M. Parlange (2010), SensorScope: Application-specific sensor network for environmental monitoring, *ACM Trans. Sens. Netw.*, 6(2), doi:10.1145/1689239.1689247.



- Koster, R. D., S. P. P. Mahanama, B. Livneh, D. P. Lettenmaier, and R. H. Reichle (2010), Skill in streamflow forecasts derived from large-scale estimates of soil moisture and snow, *Nature Geosci.*, 3(9), 613–616, doi:10.1038/ngeo944.
- Kumar, M., D. Marks, J. Dozier, M. Reba, and A. Winstral (2013), Evaluation of distributed hydrologic impacts of temperature-index and energy-based snow models, *Adv. Water Resour.*, 56(0), 77–89, doi:10.1016/j.advwatres.2013.03.006.
- 5 Lehning, M., P. Bartelt, B. Brown, T. Russi, U. Stöckli, and M. Zimmerli (1999), SNOWPACK calculations for avalanche warning based upon a new network of weather and snow stations, *Cold Reg. Sci. Technol.*, 30(1–3), 145–157, doi:10.1016/S0165-232X(99)00022-1.
- Lehning, M., I. Völksch, D. Gustafsson, T. A. Nguyen, M. Stähli, and M. Zappa (2006), ALPINE3D: a detailed model of mountain surface processes and its application to snow hydrology, *Hydrol. Proc.*, 20(10), 2111–2128, doi:10.1002/hyp.6204.
- Lehning, M., H. Löwe, M. Ryser, and N. Raderschall (2008), Inhomogeneous precipitation distribution and snow transport in steep terrain,
 10 *Water Resour. Res.*, 44(7), W07404, doi:10.1029/2007WR006545.
- Lehning, M., P. Bartelt, B. Brown, C. Fierz, and P. Satyawali (2002a), A physical SNOWPACK model for the Swiss avalanche warning Part II: Snow microstructure, *Cold Reg. Sci. Technol.*, 35(3), 147–167, doi:10.1016/S0165-232X(02)00073-3.
- Lehning, M., P. Bartelt, B. Brown, and C. Fierz (2002b), A physical SNOWPACK model for the Swiss avalanche warning Part III: Meteorological forcing, thin layer formation and evaluation, *Cold Reg. Sci. Technol.*, 35(3), 169–184, doi:10.1016/S0165-232X(02)00072-1.
- 15 Marks, D., T. Link, A. Winstral, and D. Garen (2001), Simulating snowmelt processes during rain-on-snow over a semi-arid mountain basin, *Ann. Glaciol.*, 32(1), 195–202, doi:10.3189/172756401781819751.
- Marty, C., and R. Meister (2012), Long-term snow and weather observations at Weissfluhjoch and its relation to other high-altitude observatories in the Alps, *Theor. Appl. Climatol.*, 110(4), 573–583, doi:10.1007/s00704-012-0584-3.
- Maurer, E. P., and D. P. Lettenmaier (2003), Predictability of seasonal runoff in the Mississippi River basin, *J. Geophys. Res.*, 108(D16),
 20 doi:10.1029/2002JD002555.
- Mazurkiewicz, A. B., D. G. Callery, and J. J. McDonnell (2008), Assessing the controls of the snow energy balance and water available for runoff in a rain-on-snow environment, *J. Hydrol.*, 354(1–4), 1–14, doi:10.1016/j.jhydrol.2007.12.027.
- McNamara, J. P., D. Chandler, M. Seyfried, and S. Achet (2005), Soil moisture states, lateral flow, and streamflow generation in a semi-arid, snowmelt-driven catchment, *Hydrol. Proc.*, 19(20), 4023–4038, doi:10.1002/hyp.5869.
- 25 Michlmayr, G., M. Lehning, G. Koboltschnig, H. Holzmann, M. Zappa, R. Mott, and W. Schöner (2008), Application of the Alpine 3D model for glacier mass balance and glacier runoff studies at Goldbergkees, Austria, *Hydrol. Proc.*, 22(19), 3941–3949, doi:10.1002/hyp.7102.
- Mittelbach, H., I. Lehner, and S. I. Seneviratne (2012), Comparison of four soil moisture sensor types under field conditions in Switzerland, *J. Hydrol.*, 430–431(0), 39–49, doi:10.1016/j.jhydrol.2012.01.041.
- Mott, R., F. Faure, M. Lehning, H. Löwe, B. Hynek, G. Michlmayer, A. Prokop, and W. Schöner (2008), Simulation of seasonal snow-cover distribution for glacierized sites on Sonnblick, Austria, with the Alpine3D model, *Ann. Glaciol.*, 49(1), 155–160,
 30 doi:10.3189/172756408787814924.
- Mott, R., M. Schirmer, M. Bavay, T. Grünwald, and M. Lehning (2010), Understanding snow-transport processes shaping the mountain snow-cover, *Cryosphere*, 4(4), 545–559, doi:10.5194/tc-4-545-2010.
- Nash, J., and J. Sutcliffe (1970), River flow forecasting through conceptual models part I - A discussion of principles, *J. Hydrol.*, 10(3), 282
 – 290, doi:10.1016/0022-1694(70)90255-6.
- Ochsner, T. E., R. Horton, and T. Ren (2001), A new perspective on soil thermal properties, *Soil Sci. Soc. Am. J.*, 65(6), 1641–1647, doi:10.2136/sssaj2001.1641.



- Penna, D., H. J. Tromp-van Meerveld, A. Gobbi, M. Borga, and G. Dalla Fontana (2011), The influence of soil moisture on threshold runoff generation processes in an alpine headwater catchment, *Hydrol. Earth Syst. Sci.*, 15(3), 689–702, doi:10.5194/hess-15-689-2011.
- Richards, L. (1931), Capillary conduction of liquids through porous mediums, *J. Appl. Phys.*, 1(5), 318–333, doi:10.1063/1.1745010.
- Rigon, R., G. Bertoldi, and T. M. Over (2006), GEOTop: A distributed hydrological model with coupled water and energy budgets, *J. Hydrometeor.*, 7(3), 371–388, doi:10.1175/JHM497.1.
- 5 Rössler, O., P. Froidevaux, U. Börst, R. Rickli, O. Martius, and R. Weingartner (2014), Retrospective analysis of a nonforecasted rain-on-snow flood in the Alps – a matter of model limitations or unpredictable nature?, *Hydrol. Earth Syst. Sci.*, 18(6), 2265–2285, doi:10.5194/hess-18-2265-2014.
- Schaap, M. G., F. J. Leij, and M. T. van Genuchten (2001), ROSETTA: a computer program for estimating soil hydraulic parameters with hierarchical pedotransfer functions, *J. Hydrol.*, 251(3–4), 163–176, doi:10.1016/S0022-1694(01)00466-8.
- 10 Schaefli, B., L. Nicóтина, C. Imfeld, P. Da Ronco, E. Bertuzzo, and A. Rinaldo (2014), SEHR-ECHO v1.0: a spatially explicit hydrologic response model for ecohydrologic applications, *Geosci. Model Dev.*, 7(6), 2733–2746, doi:10.5194/gmd-7-2733-2014.
- Schlögl, S., C. Marty, M. Bavay, and M. Lehning (2016), Sensitivity of Alpine3D modeled snow cover to modifications in DEM resolution, station coverage and meteorological input quantities, *Environ. Model. Softw.*, 83, 387–396, doi:10.1016/j.envsoft.2016.02.017.
- 15 Schlögl, S., R. Mott, K. Nishimura, H. Huwald, N. J. Cullen, and M. Lehning (in review), How do stability corrections perform over snow in the stable boundary layer?, *Bound.-Layer Meteor.*
- Seyfried, M. S., L. E. Grant, D. Marks, A. Winstral, and J. McNamara (2009), Simulated soil water storage effects on streamflow generation in a mountainous snowmelt environment, Idaho, USA, *Hydrol. Proc.*, 23(6), 858–873, doi:10.1002/hyp.7211.
- van Genuchten, M. T. (1980), A closed-form equation for predicting the hydraulic conductivity of unsaturated soils, *Soil Sci. Soc. Am. J.*, 20 44(5), 892–898, doi:10.2136/sssaj1980.03615995004400050002x.
- Warscher, M., U. Strasser, G. Kraller, T. Marke, H. Franz, and H. Kunstmann (2013), Performance of complex snow cover descriptions in a distributed hydrological model system: A case study for the high Alpine terrain of the Berchtesgaden Alps, *Water Resour. Res.*, 49(5), 2619–2637, doi:10.1002/wrcr.20219.
- Weingartner, R., M. Barben, and M. Spreafico (2003), Floods in mountain areas—an overview based on examples from Switzerland, *J. Hydrol.*, 25 282(1–4), 10–24, doi:10.1016/S0022-1694(03)00249-X.
- Wever, N., T. Jonas, C. Fierz, and M. Lehning (2014a), Model simulations of the modulating effect of the snow cover in a rain-on-snow event, *Hydrol. Earth Syst. Sci.*, 18(11), 4657–4669, doi:10.5194/hess-18-4657-2014.
- Wever, N., C. Fierz, C. Mitterer, H. Hirashima, and M. Lehning (2014b), Solving Richards Equation for snow improves snowpack meltwater runoff estimations in detailed multi-layer snowpack model, *Cryosphere*, 8(1), 257–274, doi:10.5194/tc-8-257-2014.
- 30 Wever, N., L. Schmid, A. Heilig, O. Eisen, C. Fierz, and M. Lehning (2015), Verification of the multi-layer SNOWPACK model with different water transport schemes, *Cryosphere*, 9(6), 2271–2293, doi:10.5194/tc-9-2271-2015.
- Wirz, V., M. Schirmer, S. Gruber, and M. Lehning (2011), Spatio-temporal measurements and analysis of snow depth in a rock face, *Cryosphere*, 5(4), 893–905, doi:10.5194/tc-5-893-2011.
- WSL Institute for Snow and Avalanche Research SLF (2015-09-29), *Meteorological and snowpack measurements from Weissfluhjoch, Davos, Switzerland*, 1, doi:10.16904/1, dataset.
- 35 Würzer, S., T. Jonas, N. Wever, and M. Lehning (2016), Influence of initial snowpack properties on runoff formation during rain-on-snow events, *J. Hydrometeor.*, 17(6), 1801–1815, doi:10.1175/JHM-D-15-0181.1.



Zappa, M., F. Pos, U. Strasser, P. Warmerdam, and J. Gurtz (2003), Seasonal water balance of an Alpine catchment as evaluated by different methods for spatially distributed snowmelt modelling, *Nord. Hydrol.*, 34(3), 179–202, doi:10.2166/nh.2003.012.



Table 1. Yearly, winter months (DJF) and summer months (JJA) precipitation sums from heated rain gauges in the area around Davos. In brackets the percentage that falls as snow, based on measured air temperature below 1.2°C.

Year	Precipitation year mm (% snow)	Precipitation DJF mm (% snow)	Precipitation JJA mm (% snow)	Precipitation year mm (% snow)	Precipitation DJF mm (% snow)	Precipitation JJA mm (% snow)
	Davos (1590 m)			Weissfluhjoch (2536 m a.s.l.)		
2011	999 (18%)	129 (76%)	410 (0%)	1767 (65%)	276 (100%)	536 (24%)
2012	1419 (36%)	547 (81%)	516 (0%)	2801 (73%)	1372 (100%)	755 (22%)
2013	1028 (24%)	223 (81%)	297 (0%)	2002 (66%)	565 (100%)	538 (39%)



Table 2. List of stations and measured quantities at the stations that are used in this study. (X): measured and used in this study, (-): not measured, (u): unventilated (temperature) or unheated (rain gauge), (v): ventilated, (h): heated rain gauge. VWC shallow denotes soil moisture sensors at 10, 30 and 50 cm depth, VWC deep denotes soil moisture sensors at 80 and 120 cm depth.

Station name	Type	Elevation (m)	TA	RH	TSS	Wind speed	Snow height	Rain gauge	ISWR	RSWR	ILWR	VWC shallow	VWC deep
Bärentalli	IMIS	2560	u	u	X	X	X	u	-	X	X	-	-
Flüelapass	IMIS	2390	u	u	X	X	X	u	-	X	X	-	-
Frauentobel	IMIS	2330	u	u	X	X	X	u	-	X	X	-	-
Gatschiefer	IMIS	2310	u	u	X	X	X	u	-	X	X	-	-
Grüniberg	IMIS	2300	u	u	X	X	X	u	-	X	X	-	-
Madrisa	IMIS	2140	u	u	X	X	X	-	-	X	X	-	-
SLF	IMIS	1560	u	u	X	X	X	-	-	X	X	X	X
Grossalp	IRKIS	1960	v	v	X	X	X	u	-	X	X	X	X
Uf den Chaiseren	IRKIS	1590	v	v	X	X	X	u	-	X	X	X	X
Dorfji	SENS ¹	1813	-	-	-	-	-	-	-	-	-	X	-
Golf Course	SENS ¹	1537	-	-	-	-	-	-	-	-	-	X	X
Pischa	SENS ¹	2156	-	-	-	-	-	-	-	-	-	X	-
Stillberg	SENS ¹	2218	-	-	-	-	-	-	-	-	-	X	-
Davos	SMN ²	1596	-	-	-	-	-	h	X	-	X	-	-
Weissfluhjoch	COMBI ³	2536	v	v	X	X	X	h	X	X	X	-	-

¹ SENS: Sensorscope station.

² SMN: SwissMetNet station (MeteoSwiss).

³ COMBI: Combination of IMIS, SwissMetNet and other instrumentation.



Table 3. List of parameters for the soil types for saturated water content (θ_s), residual water content (θ_r), the van Genuchten parameters α and n , the saturated hydraulic conductivity ($K_{\text{sat}}^{(1)}$), the density of soil particles (ρ_p), the thermal conductivity of soil particles (λ) and the specific heat of soil particles (c_p).

Name	$\theta_s^{(1)}$ ($\text{m}^3 \text{m}^{-3}$)	$\theta_r^{(1)}$ ($\text{m}^3 \text{m}^{-3}$)	$\alpha^{(1)}$ (m^{-1})	$n^{(1)}$ (-)	$K_{\text{sat}}^{(1)}$ (m s^{-1})	ρ_p (kg m^{-3})	λ $\text{W m}^{-1} \text{s}^{-1}$	c_p $\text{J kg}^{-1} \text{K}^{-1}$
Loamy sand	0.390	0.049	3.475	1.746	$1.22 \cdot 10^{-5}$	2600 ⁽²⁾	0.9 ⁽²⁾	1000 ⁽²⁾
Sandy loam	0.387	0.039	2.667	1.449	$4.43 \cdot 10^{-6}$	2600 ⁽³⁾	2.5 ⁽³⁾	801 ⁽³⁾
Silt loam	0.439	0.065	0.506	1.663	$2.11 \cdot 10^{-6}$	2700 ⁽³⁾	2.5 ⁽³⁾	871 ⁽³⁾

¹ ROSETTA class average parameters (Schaap *et al.*, 2001).

² Bachmann *et al.* (2001).

³ Ochsner *et al.* (2001).



Table 4. Land use classes and corresponding soil initialisations.

Land use class	Area (%)	Soil 0-60 cm	Soil 60-300 cm
Rock	29.2	loamy sand	loamy sand
Alpine meadow	21.1	silt loam	sandy loam
Rough pasture	15.5	silt loam	sandy loam
Mixed forest	12.9	silt loam	sandy loam
Bush	7.3	silt loam	sandy loam
Bare soil	6.0	silt loam	sandy loam
Glacier, ice, firn	3.2	ice	ice
Pasture	2.6	silt loam	sandy loam
Water	1.0	water	water
Settlements	0.8	rock	rock
Road	0.5	rock	rock
Wetland	0.1	silt loam	sandy loam
Vegetables	<0.1	silt loam	sandy loam

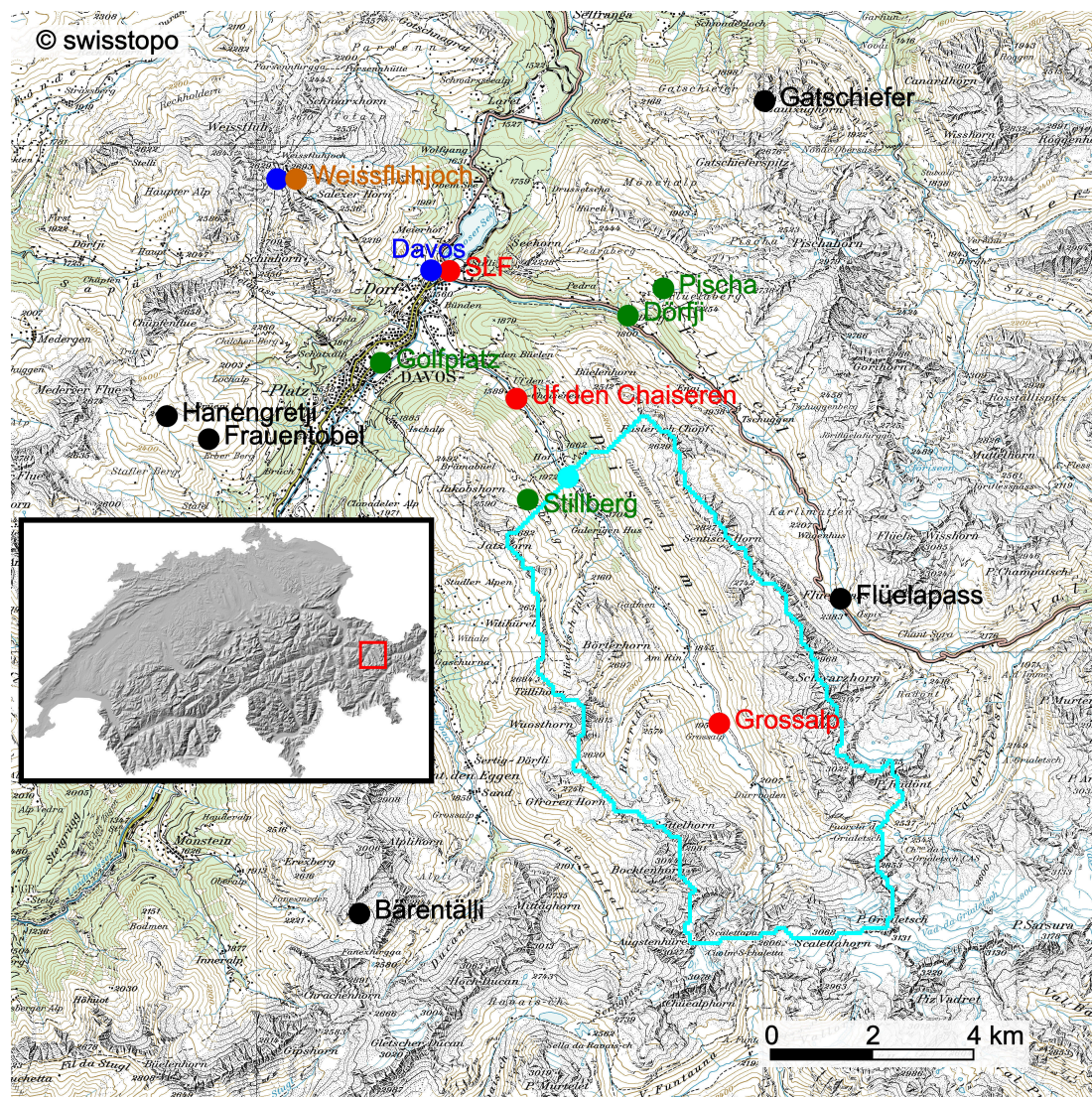
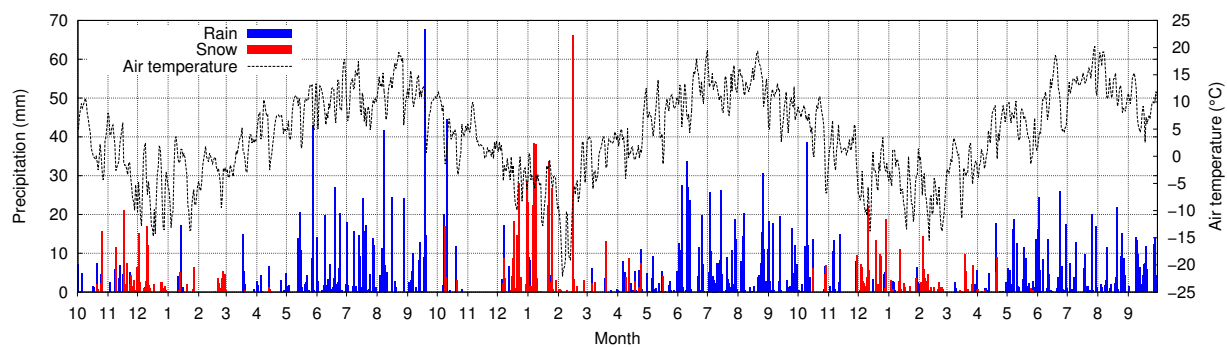
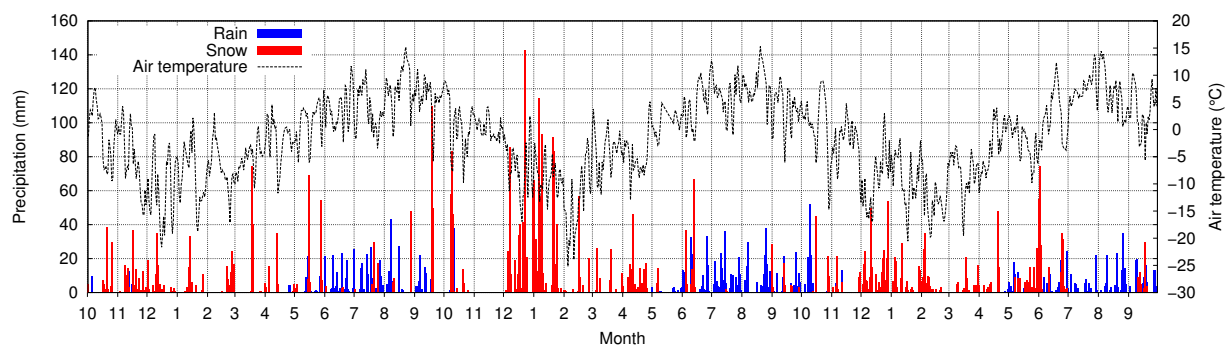


Figure 1. Topographical map of the simulated domain, showing the locations of the stations. IMIS stations are shown in black, IRKIS stations in red, SensorScope stations in green, SwissMetNet stations in blue and Weissfluhjoch in brown. The Dischma catchment and the gauging station measuring streamflow in the Dischmabach at the outlet of the Dischma catchment are shown in cyan. The inset shows the location of the simulation domain (red square) in Switzerland. Maps reproduced by permission of swisstopo (JA100118).



(a)



(b)

Figure 2. Daily rain and snowfall amounts and daily average air temperature for Davos, 1590 m (a) and Weissfluhjoch, 2536 m a.s.l. (b).

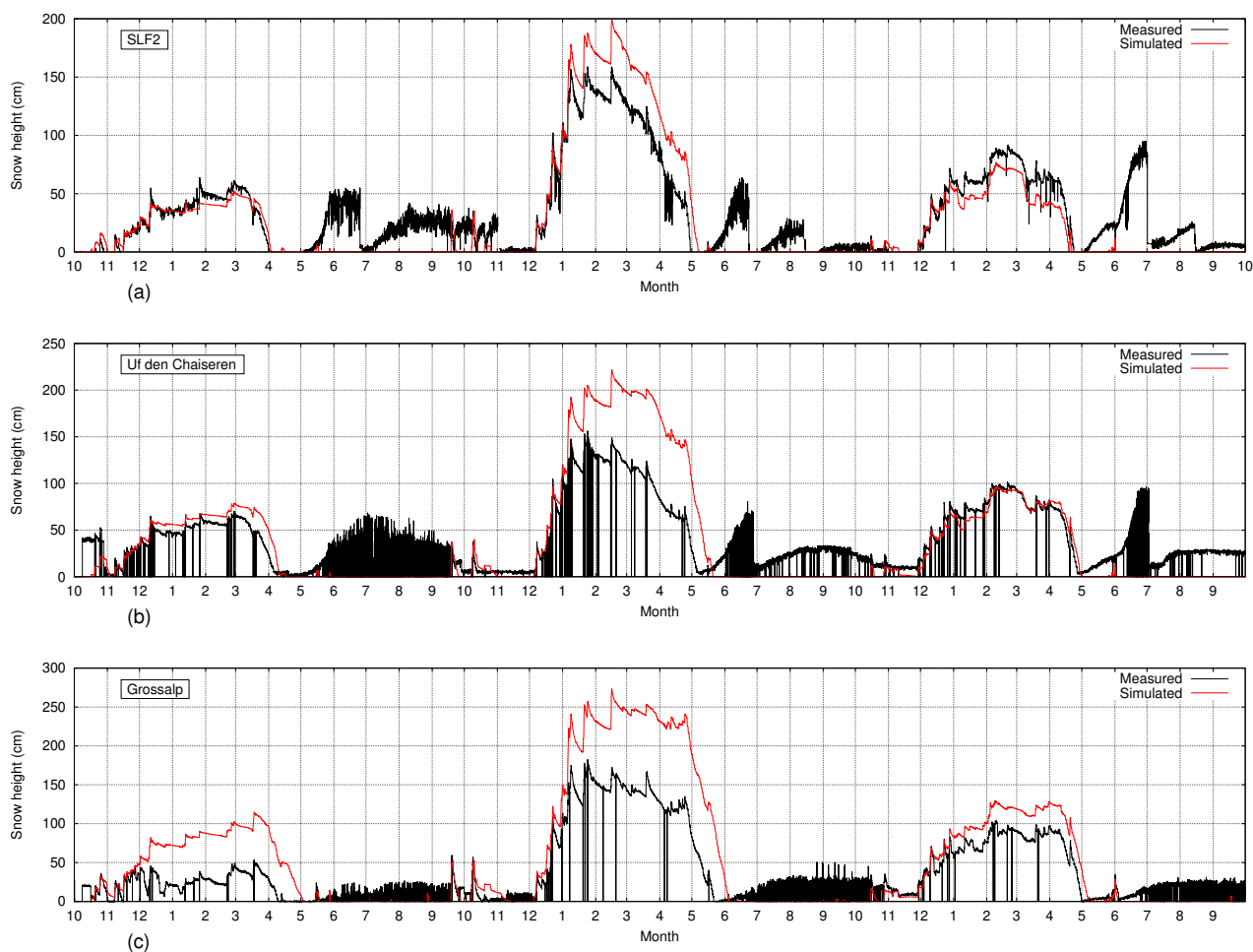


Figure 3. Measured and simulated snow depth for stations SLF2 (a), Uf den Chaiserren (b) and Grossalp (c) for the period October 2010 to October 2013.

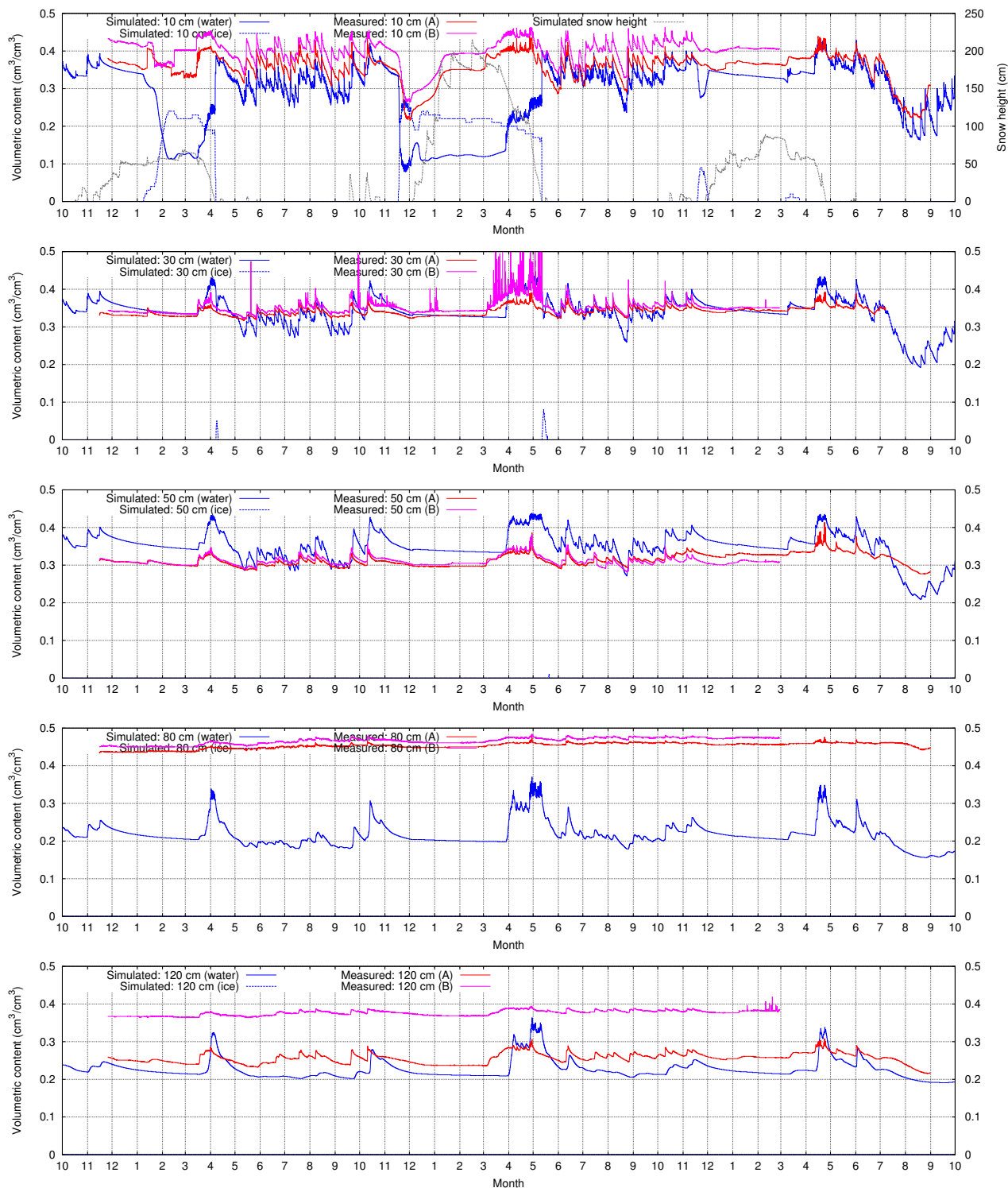


Figure 4. Measured and simulated soil moisture at the IRKIS station SLF2, for (from top to bottom) 10, 30, 50, 80 and 120 cm depth for the period October 2010 to October 2013. In the upper panel, also simulated snow height is shown.

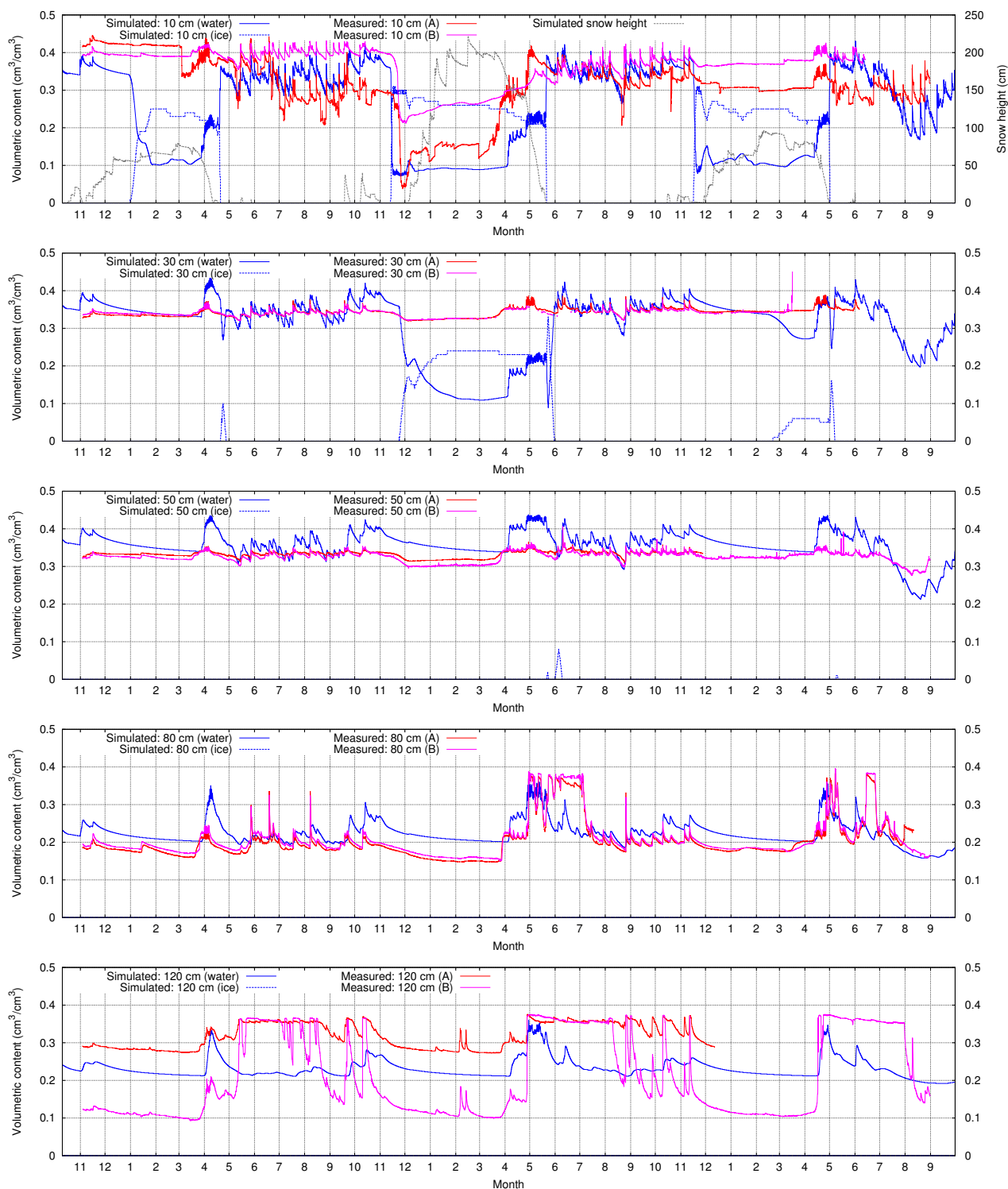


Figure 5. Measured and simulated soil moisture at the IRKIS station Uf den Chaiserren, for (from top to bottom) 10, 30, 50, 80 and 120 cm depth for the period October 2010 to October 2013. In the upper panel, also simulated snow height is shown.

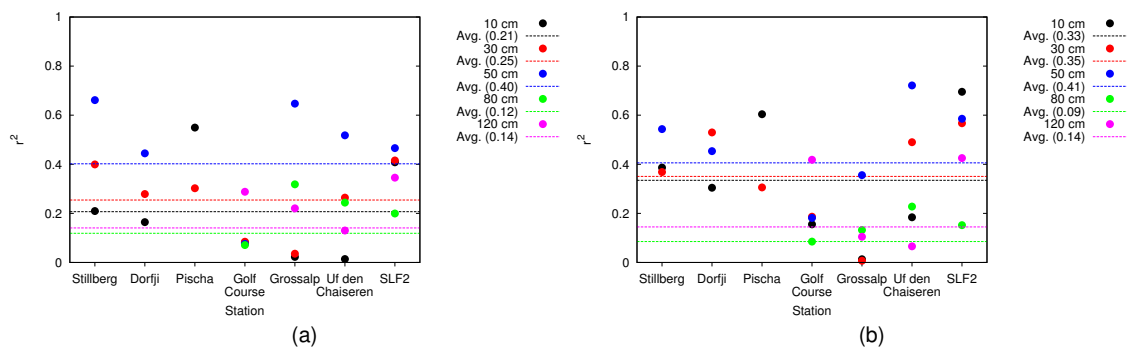


Figure 6. r^2 between measured and simulated soil moisture for the full period (a) and the summer months (b) for the 7 soil moisture stations. Dashed lines indicate the average value determined over all stations.

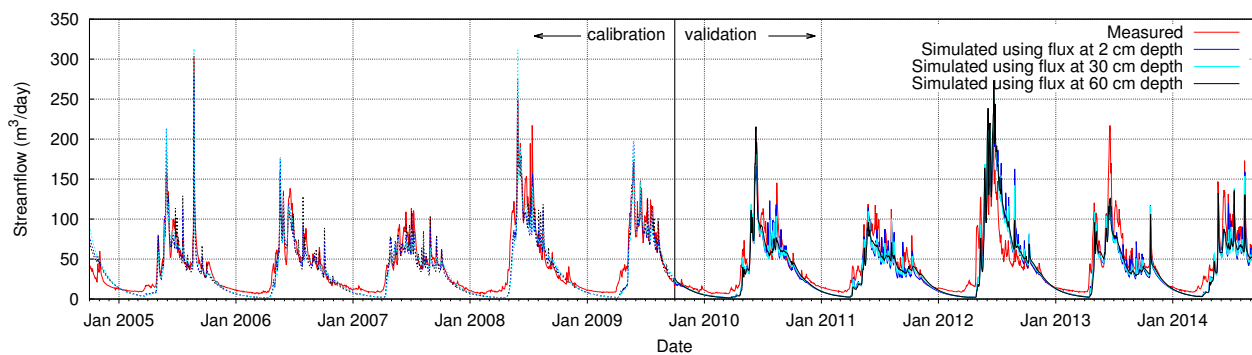


Figure 7. Measured and simulated daily streamflow for the outlet of the Dischmabach. Dashed lines denote the calibration period, solid lines denote the validation period. Major ticks on the x-axis are drawn at January 1 of each year, minor ticks are drawn at every other first of the month.

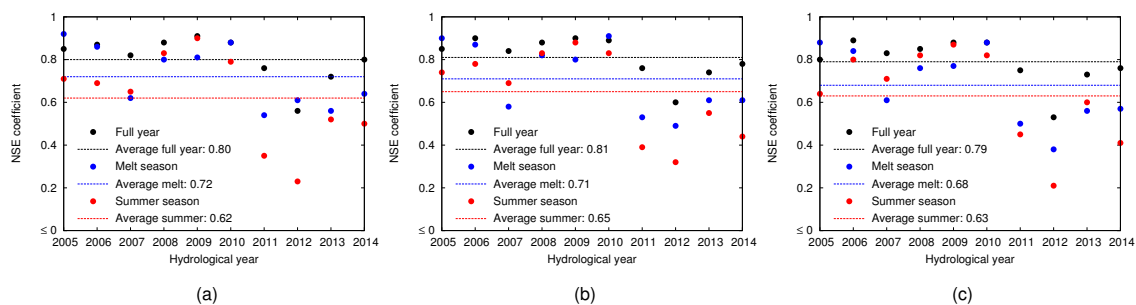


Figure 8. NSE coefficients for simulated daily streamflow for the outlet of the Dischmabach, using the 2 cm (a), 30 cm (b) or 60 cm (c) water flux in the soil layers. The NSE for the summer period for year 2012 is negative and plotted on the x-axis.

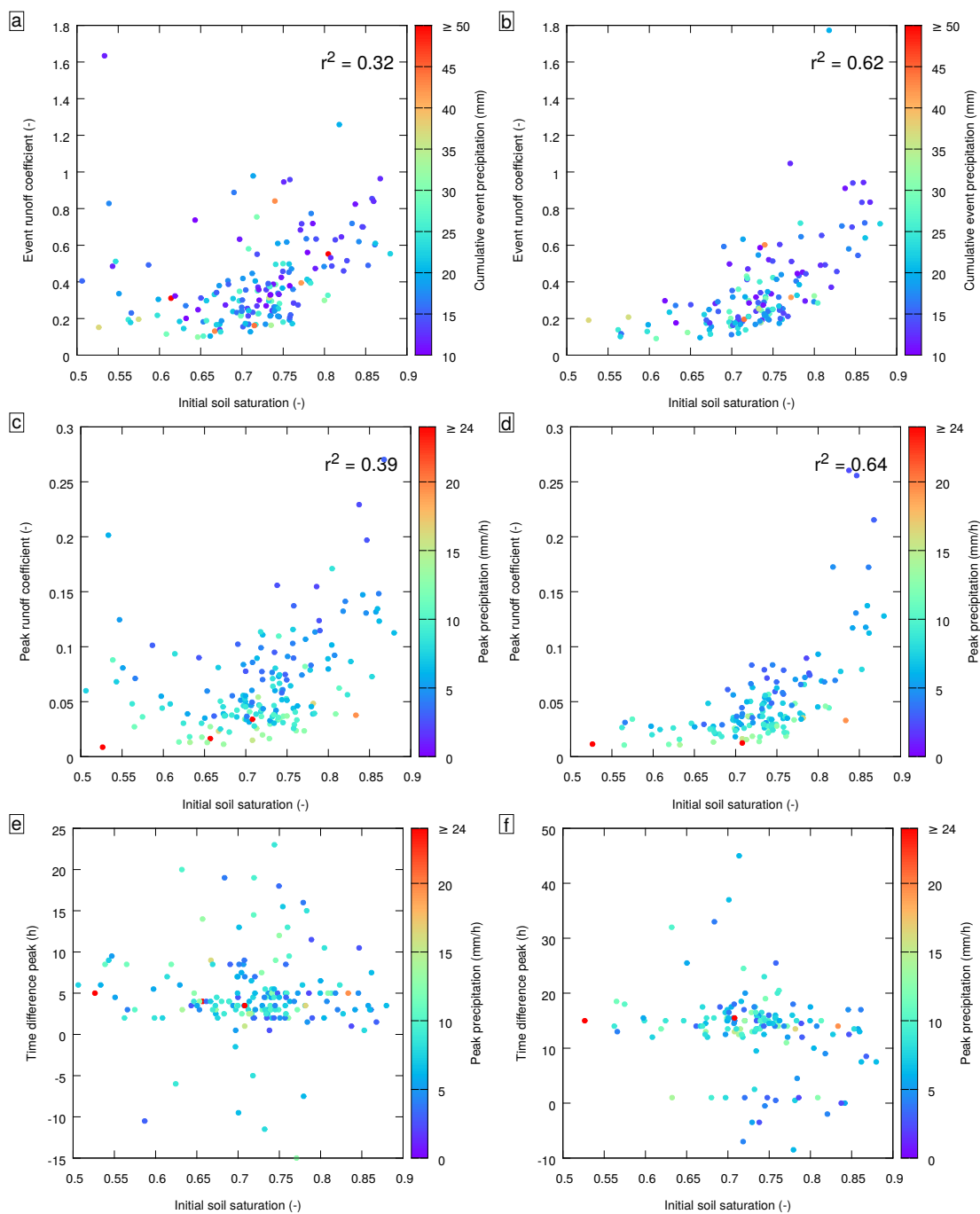


Figure 9. Rainfall event runoff coefficients for measured discharge as a function of initial soil saturation in the upper 40 cm of the soil (a) and similar for simulated discharge (b). Peak rainfall runoff coefficients for measured discharge as a function of soil saturation (c) and similar for simulated discharge (d). Time difference between peak rainfall and measured peak discharge (e) and similar for simulated peak discharge. Points are coloured according to the event rainfall sum (a and b) or the peak rainfall (c, d, e and f).

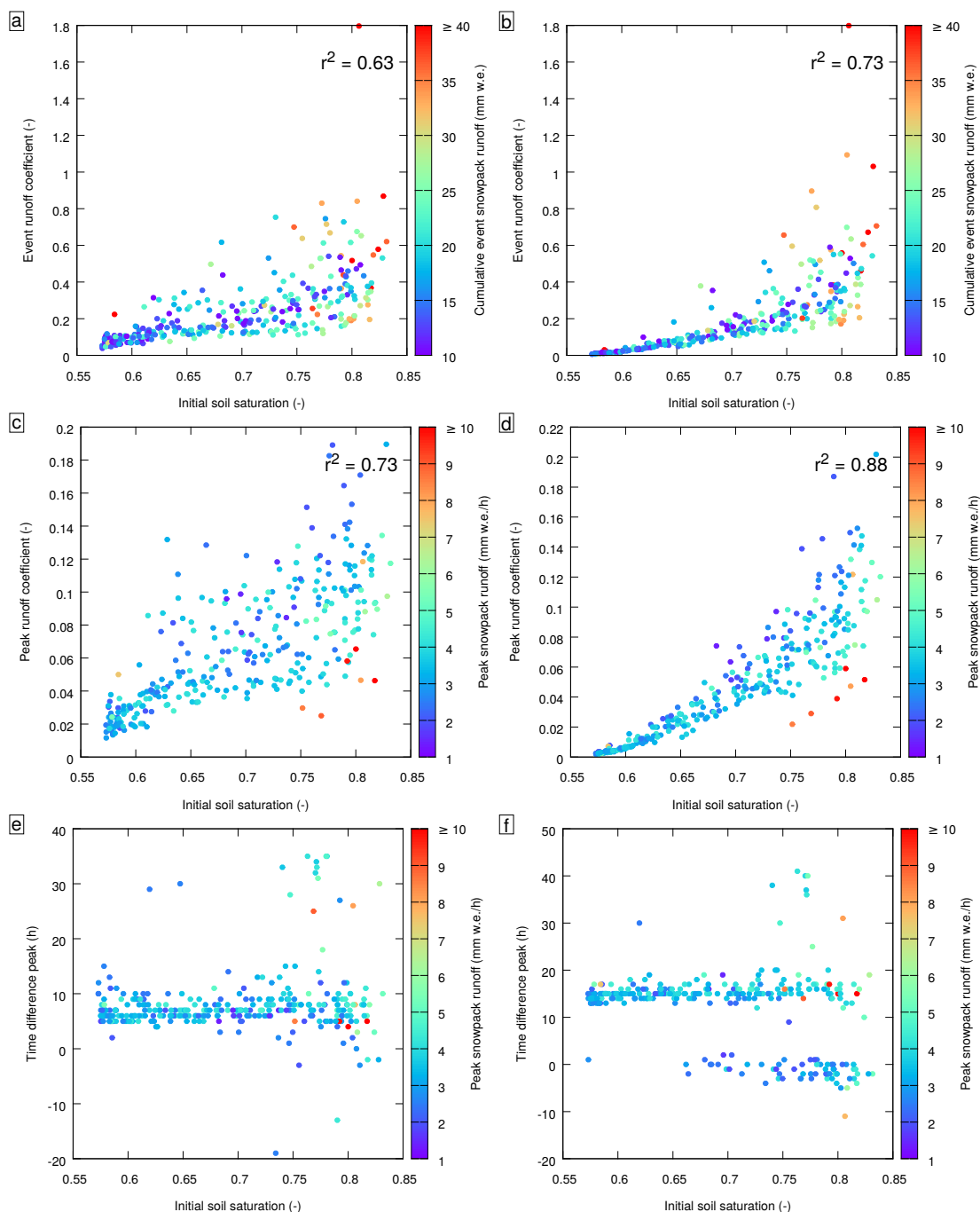


Figure 10. Snowpack runoff event runoff coefficients for measured discharge as a function of initial soil saturation in the upper 40 cm of the soil (a) and similar for simulated discharge (b). Peak snowpack runoff runoff coefficients for measured discharge as a function of soil saturation (c) and similar for simulated discharge (d). Time difference between peak snowpack runoff and measured peak discharge (e) and similar for simulated peak discharge. Points are coloured according to the event snowpack runoff sum (a and b) or the peak snowpack runoff (c, d, e and f).